

# Morphology, Rheological Behavior, and Thermal Stability of PLA/PBSA/POSS Composites

Ruyin Wang, Shifeng Wang, Yong Zhang

State Key Laboratory of Metal Matrix Composites, School of Chemistry and Chemical Technology, Shanghai Jiao Tong University, Shanghai 200240, China

Received 29 November 2008; accepted 25 February 2009

DOI 10.1002/app.30333

Published online 4 May 2009 in Wiley InterScience (www.interscience.wiley.com).

**ABSTRACT:** Octavinyl POSS (vPOSS) and epoxycyclohexyl POSS (ePOSS) were separately incorporated into the poly(lactic acid)/poly(butylene succinate-co-adipate) (PLA/PBSA) blend by melt mixing. Field emission scanning electron microscopy and X-ray diffraction analysis revealed that vPOSS existed as crystalline aggregates, whereas ePOSS was more uniformly dispersed in the composites. The storage modulus and complex viscosity slightly decreased after the addition of vPOSS, but significantly increased after the addition of ePOSS, indicating the higher melt elasticity and broader processing window of the PLA/PBSA after the addition of ePOSS. The chloroform solutions of PLA/PBSA/ePOSS composites were turbid in appearance, and the extracted POSS showed absorbant peaks assigned to the vibration of  $-\text{OH}$  and

$-\text{C}=\text{O}$  groups in the Fourier transform infrared spectroscopy analysis, indicating the reactions between ePOSS and the PLA/PBSA. Polarized optical microscopy analysis revealed that the two types of POSS could act as nucleating agents for PLA, and enhance its crystallization ability. Thermal gravimetric analysis showed that the addition of the two types of POSS increased the decomposition temperature and activation energy, consequently retarding the thermal degradation of PLA/PBSA. The retardation of degradation is more significant with the addition of ePOSS, for the reactions reduced the end groups of PLA/PBSA as well as the molecular chain mobility. © 2009 Wiley Periodicals, Inc. *J Appl Polym Sci* 113: 3095–3102, 2009

**Key words:** biodegradable; PLA; PBSA; poss; composite

## INTRODUCTION

In recent years, polyhedral oligomeric silsesquioxanes (POSS) has received much interest as a new type of nanofiller that offers the possibility of reinforcement and stabilization of polymers.<sup>1,2</sup> POSS has hybrid organic-inorganic structure characterized by the general formula of  $(\text{SiO}_{1.5})_n\text{R}_n$ , which consists of a silica cage with functional groups attached at the cage corners. The chemistry of POSS is quite flexible for it can be easily altered by chemically altering the substituent groups. POSS molecules can be incorporated into polymers through polymerization or direct blending to prepare the polymer nanocomposites. POSS with different substituents have been blended with a variety of petroleum-based polymers, such as polyolefin,<sup>3–6</sup> polystyrene,<sup>7</sup> poly(methyl methacrylate),<sup>8–10</sup> polycarbonate,<sup>11,12</sup> poly(ethylene terephthalate),<sup>2,13–15</sup> and poly(vinyl chloride)<sup>16,17</sup> to improve the mechanical properties, thermal stability, and rheological properties. For the polymer/POSS composites, how to obtain a fine and stable dispersion of POSS molecules within the poly-

mers is an important issue, which depends on the interactions between POSS substituent groups and the polymers.

Poly(lactic acid) (PLA), as a biodegradable polyester from renewable resources, has drawn great attention recently.<sup>18,19</sup> The high strength, modulus, and transparency of PLA make it a promising material for the production of environmental friendly plastics. However, the inherent brittleness of PLA is one of the disadvantages that restrict its large-scale application. Copolymerization, plasticization, and blending of PLA with flexible polymers are successful approaches to obtain the desirable mechanical properties of PLA.<sup>20–23</sup> Moreover, the low melt strength and relatively narrow processing window of PLA are the challenges in its processing and application. The degradation of PLA melt occurs with a combination of several mechanisms including ring-closing depolymerization, transesterification, thermohydrolysis, and thermo-oxidative degradation,<sup>24,25</sup> accompanied with decreasing melt strength due to the decrease in molecular weight. Some approaches such as deactivation of hydroxyl and carboxyl end groups by end capping,<sup>24,25</sup> treating PLA with peroxide or irradiation,<sup>26,27</sup> chain extension,<sup>28,29</sup> or blending with inorganic filler<sup>30–32</sup> have been adopted to improve the stability and processability of PLA. Because POSS was reported to be able to retard the changes of the thermal and

Correspondence to: Y. Zhang (yong\_zhang@sjtu.edu.cn).

Contract grant sponsor: Shanghai Leading Academic Discipline Project; contract grant number: B202.

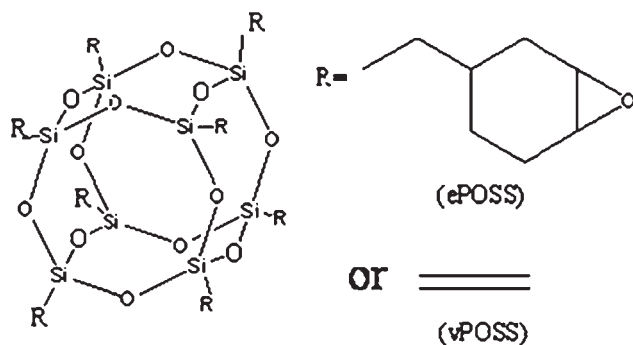


**Figure 1** Structure of polyhedral oligomeric silsesquioxanes.

rheological properties of polymers, it would be important to investigate the influence of POSS on the processability and properties of PLA based polymers.

In this study, PLA was blended with biodegradable poly(butylene succinate-co-adipate) (PBSA) at a fixed weight ratio of 70/30 for the sake of good ductility of PLA.<sup>21</sup> Octavinyl POSS and epoxy-cyclohexyl POSS were separately incorporated into the PLA/PBSA blend by melt mixing. Field emission scanning electron microscopy (FESEM) and X-ray diffraction (XRD) were used to investigate the microstructure of the nanocomposites, and polarized optical microscopy (POM) was used to observe the crystallization morphology. The thermal and rheological properties of the materials were studied using thermal gravimetric analysis (TGA) and oscillatory rheology to evaluate the stabilization. The interactions between POSS and the PLA/PBSA matrix were further investigated by the solvent extraction and Fourier transform infrared spectroscopy (FTIR) analysis.

## EXPERIMENTAL SECTION

### Materials

PLA, 3051D, was produced by Natureworks LLC., with melt flow index (MFI) of 10 g/10 min (190 °C, 2.16 kg). PBSA, EnPol G4460, was produced by IRE Chemical Co., South Korea, with MFI of 1.8 g/10 min (190 °C, 2.16 kg). The Octavinyl POSS (vPOSS), OL1160 and Epoxy-cyclohexyl POSS (ePOSS), EP0408 (Fig. 1) were purchased from Hybrid Plastic Co.

### Sample preparation

Both PLA and PBSA were dried in a vacuum oven at 60°C for 12 h before use. PLA, PBSA, and vPOSS were mixed in the mixing chamber of a Haake Rheometer RC90 at 180°C and 50 rpm for 5 min. The composites were compression molded at 180°C for 8 min, and then cold pressed for 15 min to get the sheets with the thickness of 1 mm and 3 mm for

measurements. The preparation of PLA/PBSA/ePOSS composites is slightly different. Before melt blending, a given amount of ePOSS and 5 g PLA/PBSA were mixed in chloroform solution, and the mixture was dried in a vacuum oven at 60°C for 24 h to prepare a master batch. The compositions of PLA/PBSA/POSS composites were as follows: 70/30/0, 70/30/2, 70/30/5 (weight ratio).

### Measurements

The morphology of composites was characterized by FESEM (JSM-7401F, JEOL Co., Japan). All specimens were fractured after immersion in liquid nitrogen, and coated with gold before observation.

XRD experiment was performed using an X-ray diffractometer (SA-HF3, Rigaku, Japan) equipped with a Ni-filtered Cu K $\alpha$  radiation source ( $\lambda = 0.154$  nm) at 40 KV and 40 mA from 2° to 40° at a scan rate of 4°/min.

The oscillatory rheological measurement was carried out on a rotational rheometer (Gemini 200 rheometer, Bohlin Co., UK) equipped with a parallel plate of 25 mm in diameter at 180°C and frequency range from 0.1 to 100 rad/s. Storage modulus ( $G'$ ), loss modulus ( $G''$ ), and complex viscosity ( $\eta^*$ ) were measured in the frequency sweep mode.

The FTIR spectra was obtained by using a Fourier transform infrared spectroscopy (Perkin-Elmer Paragon 1000, USA) at the resolution of 2 cm<sup>-1</sup>.

Crystallization was studied by POM (LEICA-DMLP1, Germany). A sample was melted at 180°C for 3 min and then rapidly cooled to a preset temperature for isothermal crystallization. PLA spherulites were observed in micrographs after isothermal crystallization.

TGA (Perkin-Elmer TGA7) was performed by increasing the temperature from room temperature to 600°C at a heating rate of 20°C/min under nitrogen atmosphere.

## RESULTS AND DISCUSSION

### Morphology

As seen in Figure 2(b,c), vPOSS exists in the PLA/PBSA with microaggregates and takes poor dispersion. The XRD patterns of the composites also indicate the poor dispersion of vPOSS, as shown in Figure 3. The vPOSS is a highly crystalline material and has a characteristic dominant diffraction peak at  $2\theta = 9.7^\circ$ . In the PLA/PBSA/vPOSS composites, the peak corresponding to the dominant vPOSS peak appears at 2 wt % loading and grows stronger at 5 wt % loading, indicating the presence of vPOSS crystalline aggregates in the polymer matrix. Hence, the

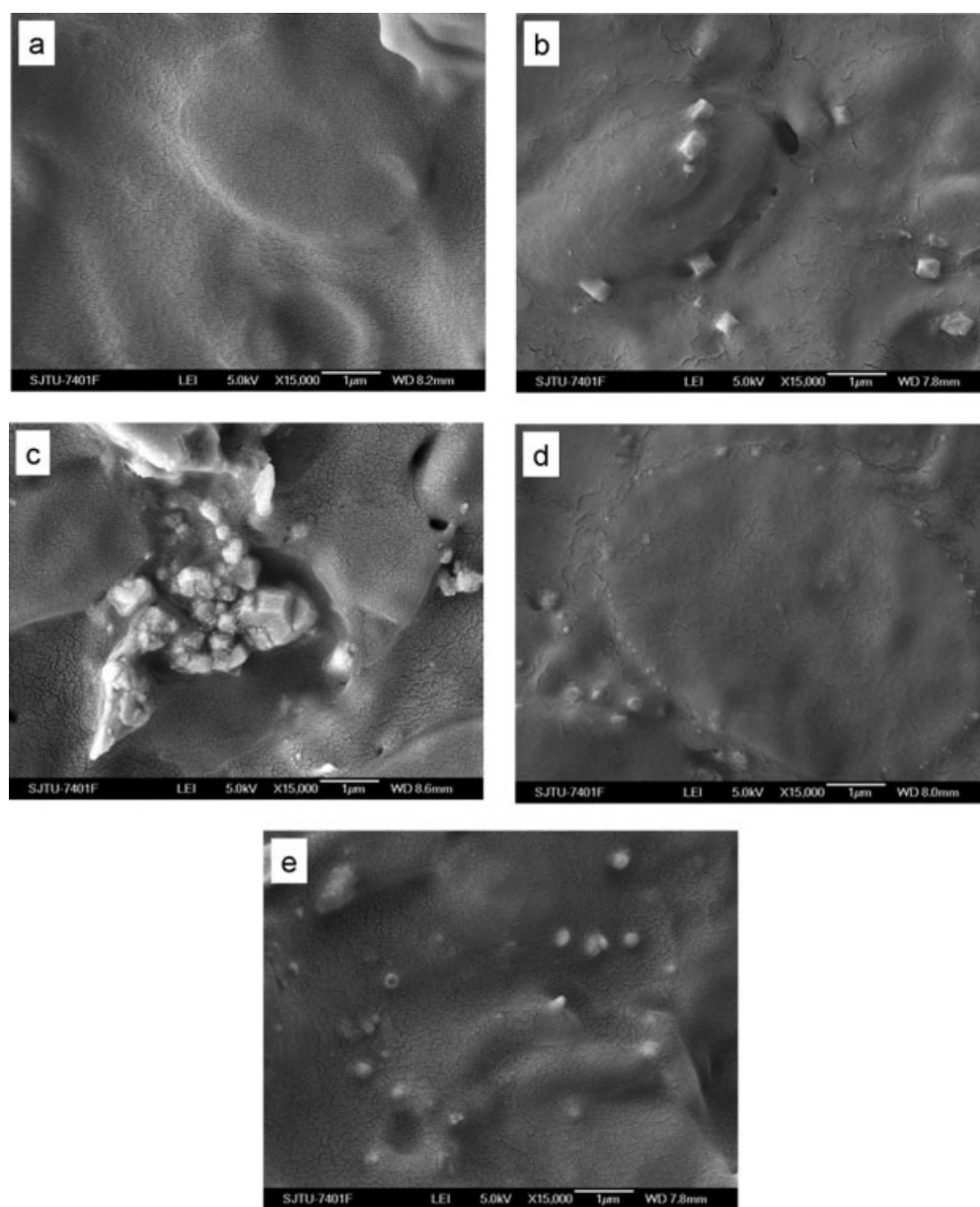


**Figure 2** FESEM micrographs of fractured surfaces of (a) PLA/PBSA and PLA/PBSA/POSS composites (b) vPOSS-2; (c) vPOSS-5; (d) ePOSS-2; (e) ePOSS-5.

vPOSS exists as crystal when it is simply mixed with the PLA/PBSA (70/30) blend.

Compared with vPOSS, ePOSS has better dispersion in the PLA/PBSA matrix [Fig. 2 (d,e)]. The ePOSS appears in the form of a viscous fluid, which does not crystallize at room temperature. So the ePOSS that is observed should be some ePOSS domains, rather than the crystalline aggregates like vPOSS. From the XRD patterns of PLA/PBSA/ePOSS composites shown in Figure 3, ePOSS shows two halos at  $2\theta = 6.3^\circ$  and  $18.2^\circ$ , corresponding to the low angle and high angle amorphous peaks of ePOSS, respectively. It has been demonstrated that the halos corresponding to the diffraction of liquid POSS could be observed if POSS is poorly distrib-

uted in polymers.<sup>6,9</sup> However, no visible peak corresponding to the diffraction of ePOSS is observed in the PLA/PBSA/ePOSS composites, indicating better dispersion of ePOSS, which coincides with the observation of FESEM.

#### Rheological behavior and FTIR analysis

$G'$ ,  $G''$ , and  $\eta^*$  versus frequency are shown in Figure 4. It can be seen that  $\eta^*$  of the composite with 2 wt % vPOSS loading is lower than that of the PLA/PBSA blend, but increase with 5 wt % vPOSS loading, and the similar results were reported in other researches.<sup>3,4</sup> The compatibility of the PLA/PBSA matrix with vPOSS at low loading likely leads to a

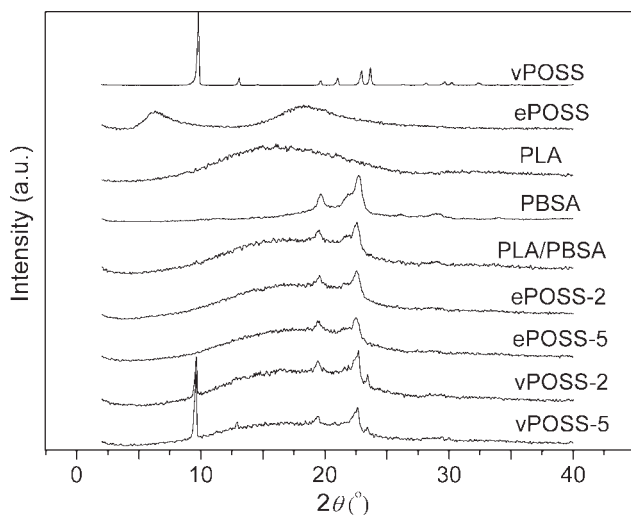


**Figure 3** XRD patterns of POSS, PLA, PBSA, and PLA/PBSA/POSS composites.

fine dispersion of vPOSS [Fig. 2(b)] with some level of physical interaction between the polymer chains and vPOSS, such as weak van der Waals forces. This interaction probably leads to decreased chain entanglement and more free volume in the melt, thus resulting in the slightly lower  $\eta^*$ . With 5 wt % vPOSS loading, the larger aggregates of crystalline vPOSS would hinder the flow of the polymer chains, thus the  $\eta^*$  increases.<sup>4</sup> It has been reported that liquid-like POSS has a plasticization effect on the rigid polymers.<sup>9,16,17</sup> Compared with the PLA/PBSA blend, PLA/PBSA/ePOSS composites with both 2 and 5 wt % loadings exhibit higher  $G'$ ,  $G''$ , and  $\eta^*$ . This should be attributed to the reactions between the epoxy groups on the ePOSS and the hydroxyl and carboxyl end groups on the PLA and PBSA molecular chains.<sup>30</sup>

Solvent extraction and ultra-centrifugation were used to investigate the solution behavior of the composites, trying to prove the reactions between ePOSS and PLA/PBSA. One gram of sample was dissolved in 30 mL chloroform to form a solution for observing their physical appearance. The solutions of PLA/PBSA/ePOSS composites are turbid in appearance, while other specimens are clear. The turbidity is attributed to the scattering of light by the suspended particles in the solutions.<sup>33</sup> Since chloroform is a good solvent for PLA, PBSA, and ePOSS, their solutions should be clear. The turbidity may be related to the crosslinked network formed by the reactions between the ePOSS and PLA/PBSA. The insoluble fraction of the PLA/PBSA/ePOSS solution was extracted with repeated cycles of washing with chloroform to completely remove the unbound polymer chains and followed by centrifugation (14,000 rpm, 5 min), and then further characterized by FTIR. As shown in Figure 5, both PLA and PBSA show the

absorption peaks around  $3450\text{ cm}^{-1}$  and  $1740\text{ cm}^{-1}$ , which are ascribed to the stretching vibration of  $-\text{OH}$  and  $-\text{C}=\text{O}$  groups. For POSS, the band at  $1109\text{ cm}^{-1}$  is assigned to the stretching vibration of  $\text{Si}-\text{O}-\text{Si}$  units in the silsesquioxane cage. Compared with ePOSS, the extracted ePOSS shows additional absorbent peaks assigned to the vibration of  $-\text{OH}$  and  $-\text{C}=\text{O}$  groups, which are due to the bounded polymer chains on the ePOSS. This implies

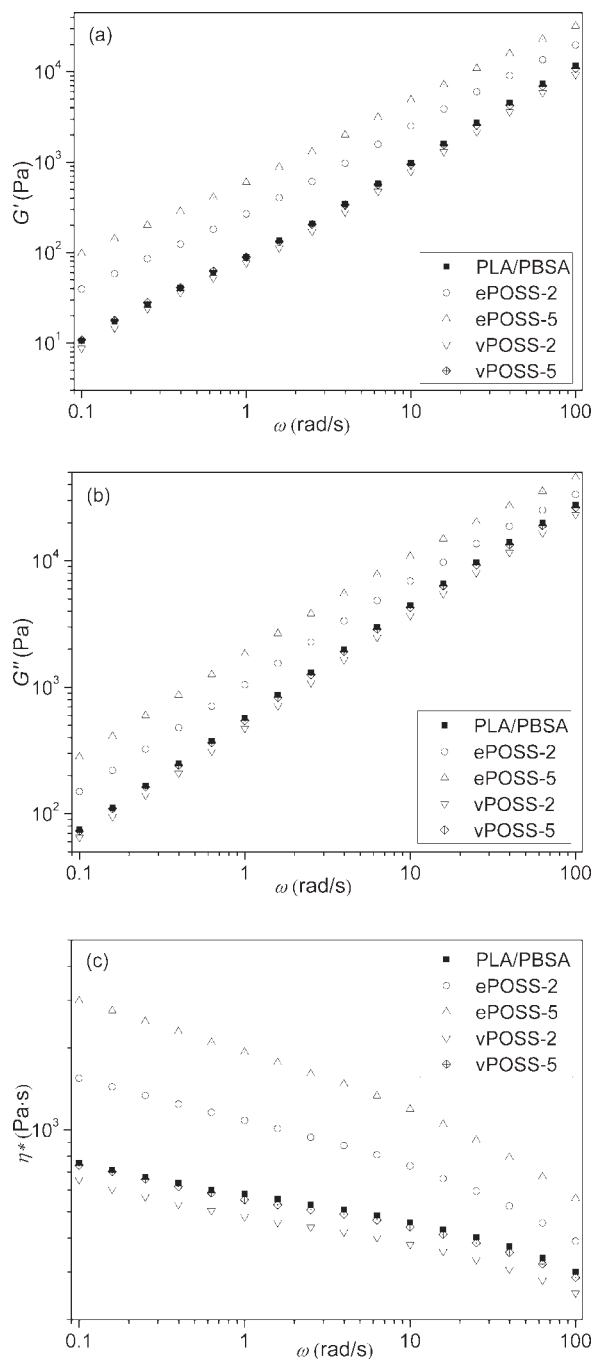


**Figure 4** (a) Storage modulus  $G'$ , (b) loss modulus  $G''$ , and (c) complex viscosity  $\eta^*$  of PLA/PBSA/POSS composites.

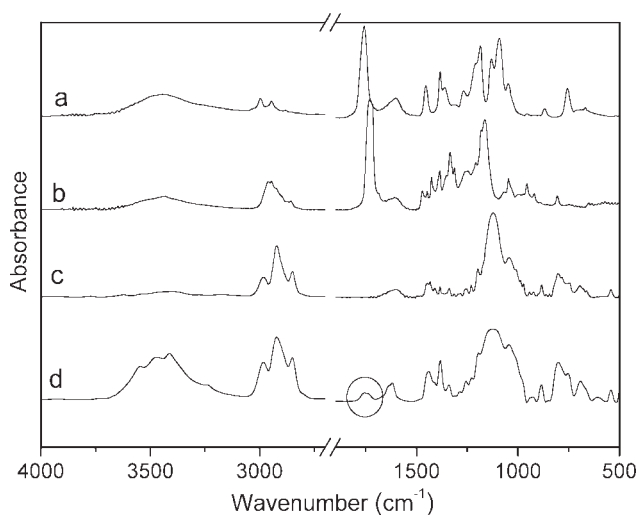


**Figure 5** The FTIR spectra of (a) PLA, (b) PBSA, (c) ePOSS, and (d) extracted ePOSS.

reactions between ePOSS and PLA/PBSA, which is closely related to the increment of the viscosity and better dispersion of ePOSS. The reactions between the epoxy groups of ePOSS and the end groups of PLA/PBSA are schematized in Figure 6.

### Spherulitic morphology

Figure 7 presents the POM micrographs of PLA, PLA/PBSA, and PLA/PBSA/POSS composites after isothermal crystallization at 120°C for 60 min. The PLA spherulites with a diameter about 100 μm can be seen, and perfectly grow with the maltese cross. After the addition of PBSA, the number and size of the PLA spherulites do not change, but the crystals become less perfect, which might be due to the interruption of the PBSA molecular chains. The addition of POSS enhances the formation of PLA crystal nucleus, as demonstrated by the increased number and the decreased diameter of the spherulites. In the PLA/PBSA/ePOSS composites, the spherulites with a cross extinction pattern could still be observed. However, a large quantity of small crystal aggregates is visible in the PLA/PBSA/vPOSS composites. These indicate that vPOSS has more significant nucleation effect on PLA than ePOSS.

### Thermal stability

The effect of POSS on the thermal stability of the PLA/PBSA matrix was evaluated by TGA (Fig. 8). Within the experimental temperature range, all the TGA curves display one stage degradation mechanism, implying that the existence of POSS does not significantly affect the degradation mechanism of the matrix polymers. The initial decomposition tempera-

ture that is defined as the temperature at 5 wt % mass loss ( $T_{5\%}$ ) and the char yield at 600°C were calculated from the curves. The integral method proposed by Horowitz and Metzger<sup>34</sup> was used to calculate the activation energy for thermal decomposition by eq. (1):

$$\ln[\ln(1/1 - \alpha)] = E_t \theta / RT_{\max}^2 \quad (1)$$

$\alpha$  is the decomposed fraction,  $E_t$  is the activation energy for decomposition,  $T_{\max}$  is the temperature at the maximum rate of weight loss, and calculated from the peak values of the differential thermogravimetric thermograms (DTA) curves,  $\theta$  is  $(T - T_{\max})$ , and  $R$  is the gas constant.  $E_t$  was calculated from the slope of the straight line of  $\ln[\ln(1/1 - \alpha)]$  versus  $\theta$ . The results are shown in Table I.

POSS shows a competition between evaporation/sublimation and decomposition when heated in nitrogen.<sup>5</sup> It can be seen that vPOSS has a  $T_{\max}$  of 333°C and a residual amount of 10% which is much lower than the amount of vPOSS inorganic fraction (66%) due to its sublimation. The PLA/PBSA blend undergoes completely weight loss with maximum rate at 425°C. For the PLA/PBSA/vPOSS composites, the  $T_{\max}$  and  $E_t$  slightly increase after the addition of vPOSS, indicating that the incorporation of vPOSS improves the thermal stability of the PLA/PBSA matrix. The stabilization is attributed to the shielding effect of the residual vPOSS component. The superficial layer produced by the degradation of vPOSS could act as a physical barrier, limiting the heat flux to the PLA/PBSA matrix and hindering the exit of the volatile degradation gases from the matrix, thus retarding the thermal decomposition of the PLA/PBSA matrix.<sup>5,6</sup> PLA/PBSA/vPOSS (70/30/5) has lower  $T_{5\%}$  than the PLA/PBSA/vPOSS (70/30/2), which might be due to partial sublimation of vPOSS,<sup>6</sup> for the vPOSS is badly entrapped in the polymer matrix at 5 wt % loading, as shown in the FESEM image [Fig. 2(c)].

Compared with vPOSS, ePOSS is much more stable and has more significant improvement of the thermal stability for the PLA/PBSA blend. This is due to the fact that besides the shielding effect of the larger amount of the residual ePOSS, the

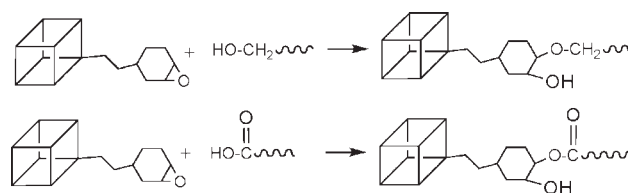


**Figure 6** Schematic illustration of the reactions between ePOSS and PLA/PBSA chains.

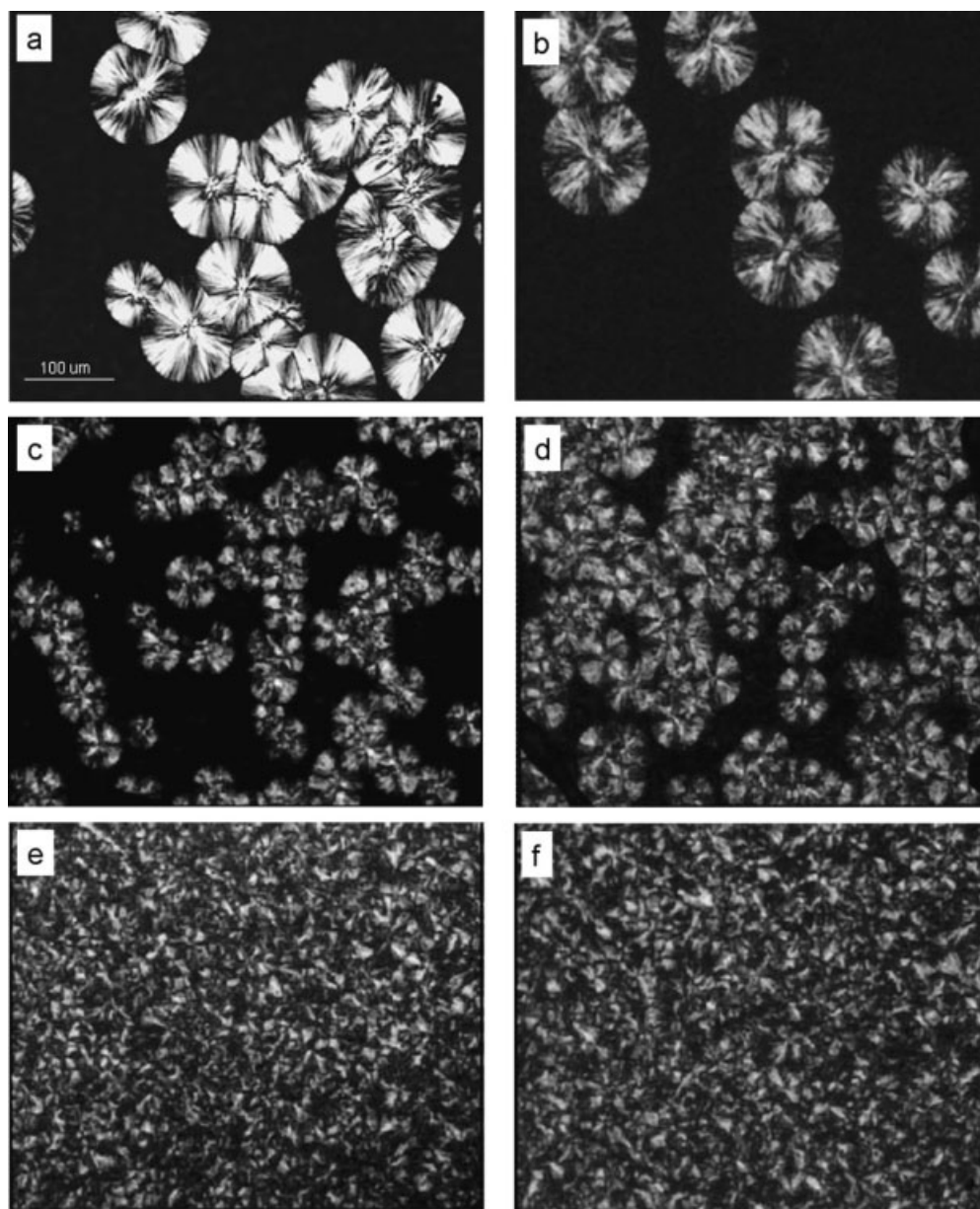


**Figure 7** Polarized optical microscopy images of (a) PLA, (b) PLA/PBSA, and PLA/PBSA/POSS composites, (c) ePOSS-2; (d) ePOSS-5; (e) vPOSS-2; (f) vPOSS-5.

reactions between the epoxy groups of ePOSS and the hydroxyl and carboxyl groups of PLA/PBSA have caused the reduction of the end groups and retardation of molecular chain motion, which both contribute to the improvement of the stabilization.<sup>2,24,25,35</sup> The composite with 2 wt % ePOSS loading is more stable than the composite at 5 wt % loading. As discussed before, the ePOSS domain at 5 wt % loading can be clearly seen in the polymer matrix, indicating that some unreacted ePOSS molecules exist in the matrix. It has been demonstrated that the self ring-opening polymerization of ePOSS occurs at 350–400 °C, which would produce free rad-

icals,<sup>36</sup> The free radicals could facilitate the chain scission and accelerate the decomposition of the molecular chains, thus resulting in the lower thermal stability.<sup>25,37</sup>

## CONCLUSIONS

Octavinyl POSS (vPOSS) and epoxycyclohexyl POSS (ePOSS) were separately incorporated into the PLA/PBSA (70/30) blend to improve the processability and thermal stability of the PLA/PBSA blend. The vPOSS existed in the PLA/PBSA blend as crystalline aggregates, whereas ePOSS dispersed more

uniformly, as determined by FESEM and XRD analysis. Compared with vPOSS, ePOSS had more significant effect on the improvement of  $G'$ ,  $G''$ , and  $\eta^*$ , indicating higher melt elasticity and broader processing window of the material after the addition of ePOSS. The reactions between the epoxy groups of ePOSS and the hydroxyl and carboxyl groups of PLA/PBSA, which are closely related to the increment of the viscosity and better dispersion of ePOSS, were confirmed by the solution behavior and FTIR analysis. The two types of POSS could act as heterogeneous nucleating agents for PLA, as demonstrated by the increased number and the decreased diameter of the crystalline spherulites. The thermal stability of the PLA/PBSA blend was improved by adding the two types of POSS as the temperature at maximum weight loss rate and decomposition activation energy of the composites increased. The stabilization became higher after the addition of ePOSS, which should be attributed to the reduced hydroxyl and carboxyl end groups and the limited molecular chain mobility resulted from the reactions.

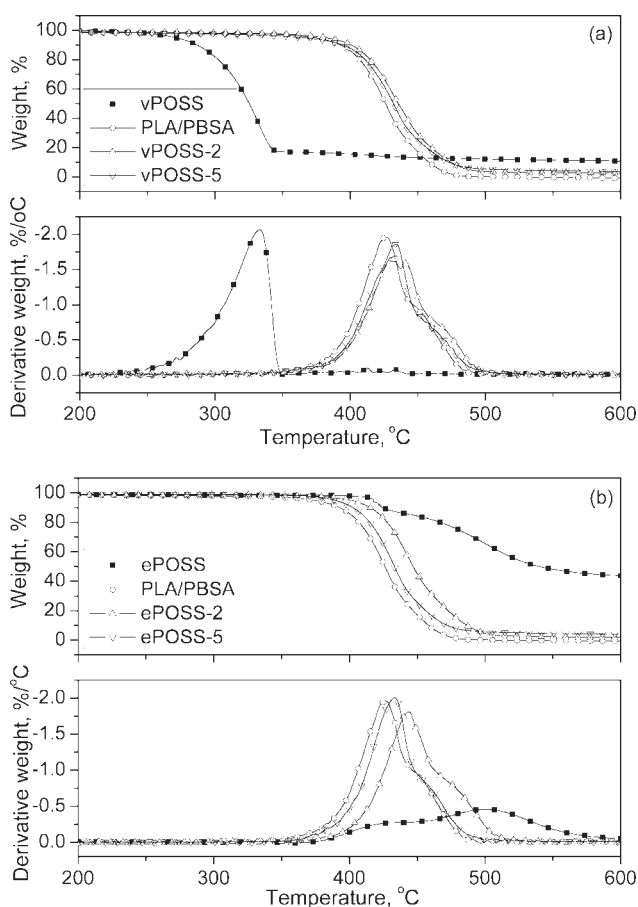


**Figure 8** TGA and DTA curves of POSS, PLA/PBSA, and PLA/PBSA/POSS composites (a) vPOSS; (b) ePOSS.

**TABLE I**  
Thermal Stability Parameters of PLA/PBSA, and PLA/PBSA/POSS Composites

Samples	$T_{5\%}$ (°C)	$T_{max}$ (°C)	$E_t$ (kJ/mol)	Char <sup>a</sup> (%)	Char <sup>b</sup> (%)
PLLA/PBSA	374	425	190	0	0
vPOSS-2	382	430	215	2.57	0.21
vPOSS-5	366	436	216	3.61	0.51
ePOSS-2	401	445	252	1.80	0.86
ePOSS-5	389	434	248	3.88	2.08

<sup>a</sup> The experimental value.

<sup>b</sup> The theoretical value.

## References

- Pielichowski, K.; Njuguna, J.; Janowski, B.; Pielichowski, J. *Adv Polym Sci* 2006, 201, 225.
- Ciolacu, F. C. L.; Choudhury, N. R.; Dutta, N.; Kosior, E. *Macromolecules* 2007, 40, 265.
- Zhou, Z.; Zhang, Y.; Zhang, Y.; Yin, N. *J Polym Sci Part B: Polym Phys* 2008, 46, 526.
- Joshi, M.; Butola, B. S.; Simon, G.; Kukaleva, N. *Macromolecules* 2006, 39, 1839.
- Fina, A.; Abbenhuis, H. C. L.; Tabuani, D.; Frache, A.; Camino, G. *Polym Degrad Stab* 2006, 91, 1064.
- Fina, A.; Tabuani, D.; Frache, A.; Camino, G. *Polymer* 2005, 46, 7855.
- Hao, N.; Bohning, M.; Schonhals, A. *Macromolecules* 2007, 40, 9672.
- Kopesky, E. T.; McKinley, G. H.; Cohen, R. E. *Polymer* 2006, 47, 299.
- Kopesky, E. T.; Haddad, T. S.; McKinley, G. H.; Cohen, R. E. *Polymer* 2005, 46, 4743.
- Kopesky, E. T.; Haddad, T. S.; Cohen, R. E.; McKinley, G. H. *Macromolecules* 2004, 37, 8992.
- Song, L.; He, Q.; Hu, Y.; Chen, H.; Liu, L. *Polym Degrad Stab* 2008, 93, 627.
- Zhao, Y.; Schiraldi, D. A. *Polymer* 2005, 46, 11640.
- Zeng, J.; Kumar, S.; Iyer, S.; Schiraldi, D. A.; Gonzalez, R. I. *High Perform Polym* 2005, 17, 403.
- Yoon, K. H.; Polk, M. B.; Park, J. H.; Min, B. G.; Schiraldi, D. A. *Polym Int* 2005, 54, 47.
- Vannier, A.; Duquesne, S.; Bourbigot, S.; Castrovinci, A.; Camino, G.; Delobel, R. *Polym Degrad Stab* 2008, 93, 818.
- Soong, S. Y.; Cohen, R. E.; Boyce, M. C. *Polymer* 2007, 48, 1410.
- Soong, S. Y.; Cohen, R. E.; Boyce, M. C.; Mulliken, A. D. *Macromolecules* 2006, 39, 2900.
- Drumright, R. E.; Gruber, P. R.; Henton, D. E. *Adv Mater* 2000, 12, 1841.
- Lunt, J. *Polym Degrad Stab* 1998, 59, 145.
- Lin, Y.; Zhang, K. Y.; Dong, Z. M.; Dong, L. S.; Li, Y. S. *Macromolecules* 2007, 40, 6257.
- Shibata, M.; Teramoto, N.; Inoue, Y. *Polymer* 2007, 48, 2768.
- Auras, R.; Harte, B.; Selke, S. *Macromol Biosci* 2004, 4, 835.
- Chigwada, G.; Jash, P.; Jiang, D. D.; Wilkie, C. A. *Polym Degrad Stab* 2005, 89, 85.
- Brostrom, J.; Boss, A.; Chronakis, I. S. *Biomacromolecules* 2004, 5, 1124.
- Kopinke, F. D.; Remmler, M.; Mackenzie, K.; Moder, M.; Wachsen, O. *Polym Degrad Stab* 1996, 53, 329.
- Quynh, T. M.; Mitomo, H.; Nagasawa, N.; Wada, Y.; Yoshii, F.; Tamada, M. *Eur Polym J* 2007, 43, 1779.
- Semba, T.; Kitagawa, K.; Ishiaku, U. S.; Hamada, H. *J Appl Polym Sci* 2006, 101, 1816.

28. Cicero, J. A.; Dorgan, J. R.; Dec, S. F.; Knauss, D. M. *Polym Degrad Stab* 2002, 78, 95.
29. Lehermeier, H. J.; Dorgan, J. R. *Polym Eng Sci* 2001, 41, 2172.
30. Chen, Q.; Xu, R.; Zhang, J.; Yu, D. *Macromol Rapid Commun* 2005, 26, 1878.
31. Sinha Ray, S.; Maiti, P.; Okamoto, M.; Yamada, K.; Ueda, K. *Macromolecules* 2002, 35, 3104.
32. Pluta, M.; Jeszka, J. K.; Boiteux, G. *Eur Polym J* 2007, 43, 2819.
33. Bhardwaj, R.; Mohanty, A. K. *Biomacromolecules* 2007, 8, 2476.
34. Horowitz, H. H.; Metzger, G. *Anal Chem* 1963, 35, 1464.
35. Liu, Y. R.; Huang, Y. D.; Liu, L. *Polym Degrad Stab* 2006, 91, 2731.
36. Choi, J.; Yee, A. F.; Laine, R. M. *Macromolecules* 2003, 36, 5666.
37. Nugroho, P.; Mitomo, H.; Yoshii, F.; Kume, T. *Polym Degrad Stab* 2001, 72, 337.